Proc. Natl. Acad. Sci. USA
Vol. 92, pp. 3303–3307, April 1995
Physiology

Extracellular pH regulation in microdomains of colonic crypts: Effects of short-chain fatty acids

(laser scanning confocal microscopy/crypts of Lieberkühn/mouse/carboxy SNARF-1/pH microclimate)

SHAOYOU CHU AND MARSHALL H. MONTROSE*

Division of Gastroenterology, Departments of Medicine and Physiology, Johns Hopkins University School of Medicine, Baltimore, MD 21205

Communicated by John W. Littlefield, Johns Hopkins University, Baltimore, MD, December 21, 1994

ABSTRACT **It has been suggested that transepithelial gradients of short-chain fatty acids (SCFAs; the major anions in the colonic lumen) generate pH gradients across the colonic epithelium. Quantitative confocal microscopy was used to study extracellular pH in mouse distal colon with intact epithelial architecture, by superfusing tissue with carboxy SNARF-1 (a pH-sensitive fluorescent dye). Results demonstrate extracellular pH regulation in two separate microdomains surrounding colonic crypts: the crypt lumen and the subepithelial tissue adjacent to crypt colonocytes. Apical superfusion with (*i*) a poorly metabolized SCFA (isobutyrate), (*ii*) an avidly metabolized SCFA (*n*-butyrate), or (*iii*) a physiologic mixture of acetate/propionate/*n*-butyrate produced similar results: alkalinization of the crypt lumen and acidification of subepithelial tissue. Effects were (*i*) dependent on the presence and orientation of a transepithelial SCFA gradient, (*ii*) not observed with gluconate substitution, and (*iii*) required activation of sustained vectorial acid/base transport by SCFAs. Results suggest that the crypt lumen functions as a pH microdomain due to slow mixing with bulk superfusates and that crypts contribute significant buffering capacity to the lumen. In conclusion, physiologic SCFA gradients cause polarized extracellular pH regulation because epithelial architecture and vectorial transport synergize to establish regulated microenvironments.**

The large intestine contributes to water and salt conservation, in part by mediating vectorial absorption of sodium and short-chain fatty acids (SCFAs) from the colonic lumen (1). SCFAs (e.g., acetate, propionate, and butyrate) are produced by bacterial fermentation and are predominant anions (collectively 100–150 mM) in the colonic lumen (2, 3). SCFAs are a major metabolic substrate for colonocytes (2). In addition, SCFAs stimulate electroneutral sodium absorption via activation of colonocyte apical Na^+/H^+ exchange (4–7). SCFAs acidify cultured and native colonocytes (8–11), and intracellular acidification has been presumed to mediate activation of apical Na^+/H^+ exchange by SCFAs (4–8). However, recent evidence suggests that apical-to-basolateral transepithelial SCFA gradients, such as those existing *in vivio* (3), are required for efficient activation of apical Na^+/H^+ exchange (8). Basolateral SCFAs cause cellular acidification (8) but do not efficiently activate apical Na^+/H^+ exchange in HT29-18-C_1 cells (8) or stimulate sodium absorption in native tissue (5, 6, 12). To reconcile all observations, we hypothesized that transepithelial SCFA gradients generate asymmetries of intracellular and/or extracellular pH across the epithelium (8).

Consistent with this hypothesis, evidence suggests that regulation of extracellular pH may not be the same at the apical and basolateral membranes of epithelia. Extracellular pH electrodes detect a "pH microclimate" (defined as a region with a pH distinct from the bulk extracellular fluid) near the luminal surface of the colonic epithelium (13, 14). At present there is no consensus whether this space is regulated by luminal fluid pH or [SCFA] (13–15). Recent information also shows that lateral intercellular spaces between cultured renal cells (Madin–Darby canine kidney) maintain a pH distinct from bulk perfusates (16, 17). A similar basolateral pH microenvironment has been suggested for enterocytes, on the basis of mathematical modeling of transepithelial SCFA fluxes (18, 19). In this report, confocal microscopy has been applied to measure extracellular pH in crypts of mouse distal colon. Results show dynamic and polarized regulation of extracellular pH in two separate microdomains adjacent to crypt colonocytes.

MATERIALS AND METHODS

Tissue Preparation. CD-1 mice (Charles River Breeding Laboratories) were euthanized with halothane; then distal colon was excised, flushed with saline, and stripped of muscle layers. Mucosal sheets were kept at 4°C in Dulbecco's minimum Eagle's medium (GIBCO/BRL) until use. For experiments, mucosa was mounted in a chamber allowing separate perfusion of the apical (mucosal) and basolateral (serosal) surfaces while tissue was mounted on an inverted microscope (Zeiss Axiovert) coupled to a confocal laser scanning unit (Bio-Rad MRC-600). The serosal surface was closest to the microscope objective (Leitz PlanFluotar 100×; numerical aperture, 1.2; water immersion). The chamber was continuously perfused with room temperature solutions at 0.5–1 ml/min (chamber volumes: 25 μl, apical; 15 μl, basolateral). The chamber was custom manufactured (Summit Precision Machining, Baltimore) and is a modification of our microscopy chamber for study of polarized functions in cultured epithelia (8, 20). In brief, a ring secures tissue in an aluminum block with separate ports for apical and basolateral perfusion. A detailed description and validation of the chamber will be published elsewhere (unpublished data).

Perfusate Solutions. Perfusate solutions were based on a standard NaCl medium (containing in mM: 130 NaCl, 5 KCl, 1 $MgSO_4$, 2 $CaCl_2$, 20 Hepes, and 25 mannose). SCFA media substituted 130 mM NaCl in NaCl medium with 130 mM of either (sodium salts) *n*-butyrate, isobutyrate, or a mixture of the major physiologic SCFAs in mouse colon (final concentrations in mM; acetate/propionate/*n*-butyrate = 91:13:26) (14). Gluconate medium substituted 130 mM NaCl with 130 mM sodium gluconate. To make NaCl media of different buffering capacity, NaCl was reduced to 100 mM, and 20 mM Hepes was replaced by either (*i*) 5 mM Hepes plus 42 mM sodium gluconate (low buffering capacity) or (*ii*) 60 mM Hepes (high buffering capacity). To examine effects of SCFAs in media with different buffering capacity, 100 mM sodium isobutyrate was substituted for 100 mM NaCl in either the low

The publication costs of this article were defrayed in part by page charge payment. This article must therefore be hereby marked "*advertisement*" in accordance with 18 U.S.C. §1734 solely to indicate this fact.

Abbreviation: SCFA, short-chain fatty acid.

*To whom reprint requests should be addressed at: Johns Hopkins University, Ross 930, 720 Rutland Avenue, Baltimore, MD 21205.

or the high buffering capacity formulation described above. All media were isosmotic with original NaCl medium (range, 300–309 mosM; Wescor 5500 osmometer). All solutions were titrated to pH 7.4 and, unless indicated otherwise, contained 0.1 mM carboxy SNARF-1 free acid (Molecular Probes).

Measurement of Extracellular pH. Tissue was rapidly superfused with medium containing 0.1 mM carboxy SNARF-1 throughout the experiment (21). A Kr/Ar laser (488 nm) was excitation source, and two fluorescence images were collected simultaneously at 580 ± 15 nm and 640 ± 17 nm. Photobleaching of extracellular SNARF-1 was not observed. To equalize *z*-axis resolution between channels, confocal pinholes of each detector were set to equal values. *xy* images were collected under conditions of constant detector gain and dark current, from a single plane of focus in the tissue. Ratio (640 nm/580 nm) images were formed by linear division of background-corrected images (background images from chambers without dye). To optimize reliability of ratio data, image masking discarded (set to zero) ratio values calculated from regions of 580 nm or 640 nm images that had values below a preselected threshold, and regions with values of 255 (considered off-scale) were manually discarded during analysis. To analyze ratio images, mean pixel intensity was calculated from the entire lumen or a (manually selected) 3- to 5-μm band of lamina propria directly encircling the crypt basal surface (referred to as submucosal tissue). Extracellular pH was calculated from a calibration curve determined in the confocal microscope with 0.1 mM SNARF-1 in NaCl media of pH 6.0–8.0. A single point (pH 7.0) calibration was performed for each experiment to standardize pH calculation for daily instrument settings.

RESULTS

The colonic epithelium has complex three-dimensional architecture: a relatively flat surface epithelium continuous with crypt epithelium lining abundant glandular structures in the tissue. Confocal microscopy was used to visualize extracellular dye in crypt lumens (fluid spaces continuous with the colonic lumen) and submucosal tissue between crypts. Fig. 1 shows confocal images visualizing two crypts in cross section. As shown in the raw fluorescence image of Fig. 1*i*, dye penetrated into the lumen and submucosa but did not accumulate within colonocytes. By enhancing contrast in the images, dye was always detectable in lateral intercellular spaces (Fig. 1*ii*), suggesting that dye entered spaces directly adjacent to crypt colonocytes. Dual-emission ratios of SNARF-1 fluorescence were used to estimate extracellular pH (21) in the crypt lumen and submucosal tissue directly surrounding crypts. Lateral intercellular spaces may function as a distinct extracellular pH microdomain (16, 17). However, in our preparation, lateral spaces had insufficient signal for reliable ratio calculations in most experiments and therefore were not analyzed.

Experiments measured extracellular pH following exposure to luminal superfusate containing the major physiologic SCFAs in mouse colon (22). As shown qualitatively in SNARF-1 ratio images of Fig. 1 *iii–v*, apical perfusion with SCFAs reversibly alkalinized crypt lumens and acidified submucosal tissue. Results from multiple crypts are quantified in Fig. 2.

Fig. 2 also compares the physiologic SCFA mixture versus the response to equimolar concentrations of individual SCFAs that are either poorly (isobutyrate) or avidly (*n*-butyrate) metabolized by colonocytes (23–25). Fig. 2 *A* and *B* separately compile measurements of luminal pH and submucosal pH, respectively, from the same crypts. As shown, results are qualitatively similar among tested SCFAs, suggesting that SCFA metabolism is not the major basis for observations. In contrast, extracellular pH is unaffected when 130 mM chloride is replaced by equimolar gluconate. This suggests that addition of luminal SCFA, not removal of chloride, is responsible for extracellular pH regulation.

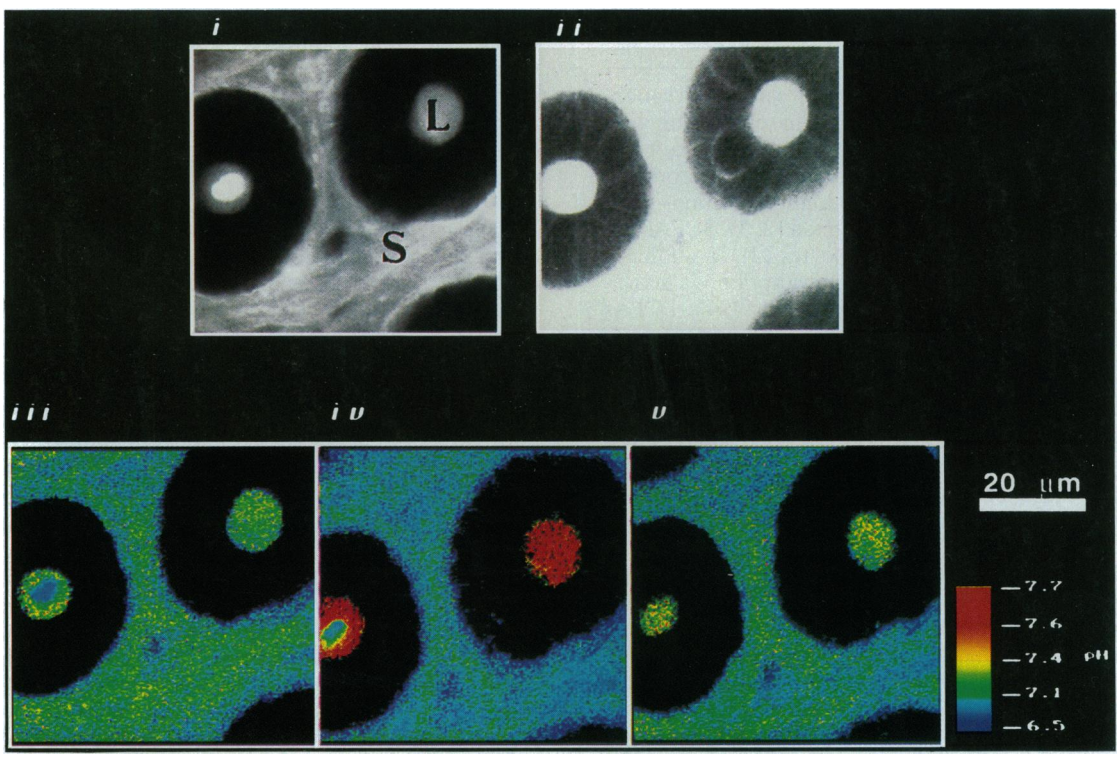

FIG. 1. Raw fluorescence and ratio images of extracellular SNARF-1 in colonic crypts. (*i*) Raw 640-nm *xy* image of crypt cross section showing SNARF-1 excluded from colonocytes but penetrating into spaces surrounding colonocytes, including central crypt lumen (L) and submucosal tissue (S) surrounding crypts. (*ii*) Same image after contrast enhancement. Pseudocolored ratio images (640 nm/580 nm) collected from the same crypts are shown in images *iii–v*, with pH values in pseudocolor scale. (*iii*) Ratio image of epithelium in NaCl medium. (*iv*) Ratio image 5 min after apical exposure to 130 mM mixed SCFAs (see text). (*v*) Ratio image 5 min after apical perfusion switched back to NaCl medium.

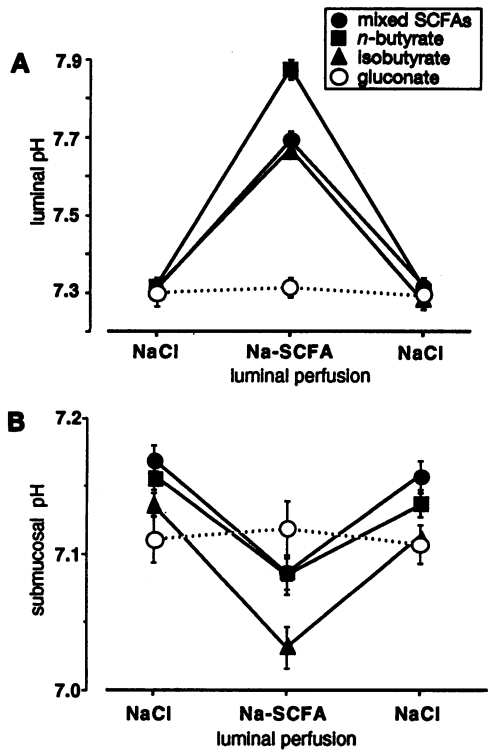

FIG. 2. Effect of luminal SCFAs on extracellular pH of mouse colonic crypts. (*A*) Analysis of luminal pH from 20 crypts in four experiments performed as in Fig. 1. Results are mean ± SEM ($n = 20$) for crypts exposed to mixed SCFAs, isobutyrate, *n*-butyrate, or gluconate. Gluconate was not significantly different from either beginning or end control (ANOVA, $P > 0.1$), but all other monocarboxylates alkalinized luminal pH significantly versus either beginning or end controls ($P < 0.0001$). (*B*) Analysis of submucosal pH from the same experiments as in *A*. All apical SCFAs (except gluconate) significantly acidified submucosal tissue ($P < 0.05$) versus controls.

Experiments tested whether results were affected by the transepithelial SCFA gradient that exists *in vivo* and in our initial protocol. Isobutyrate was used in all further experiments to minimize metabolic effects. Fig. 3*A* compiles time course experiments in which crypts were sequentially exposed to isobutyrate in basolateral and/or apical perfusates, and resultant luminal and submucosal pH values were analyzed separately. Ratio images in Fig. 3*B* were collected from a single experiment, at times indicated by markers in Fig. 3*A*. As shown, reversing orientation of the transepithelial SCFA gradient produces qualitatively opposite changes in luminal and submucosal pH (compare *ii* versus *iv*). This suggests that all transepithelial acid/base transport mechanisms that contribute to polarized pH changes are readily reversible. Bilateral perfusion with identical isobutyrate solutions (*iii*) produces minimal changes in extracellular pH versus the NaCl condition (*i*). This suggests that transepithelial SCFA gradients, and not just presence of SCFAs, are required to generate polarized extracellular pH changes. This strongly supports transport, and not SCFA metabolism, as the basis for observations.

Experiments addressed how crypt lumens maintain pH distinct from bulk perfusate pH. Experiments first measured the time course of SNARF-1 dye entry into crypts. Then, in the presence of constant extracellular SNARF-1, apical SCFA was added and resultant luminal pH changes were monitored at the same location. As shown in Fig. 4, dye entered crypt lumens with a $t_{1/2} \approx 2$ min and apical SCFA addition changed luminal pH with a similar time course. In contrast, control experiments demonstrated that within 30 sec (*i*) apical dye fully equilibrated in the bulk perfusate directly adjacent to tissue and (*ii*) basolateral dye fluorescence reached steady state in submucosal tissue (data not shown). The experiment suggests that entry of SCFAs into crypt lumens may be rate limiting for observed pH changes. More importantly, a restricted mixing environment in crypt lumens explains how a luminal pH microdomain is maintained, despite continuity of crypt luminal fluid with colonic luminal fluid.

To explore why transepithelial SCFA gradients were required to regulate extracellular pH, experiments compared response to apical media of different buffering capacity in either the presence or the absence of 100 mM isobutyrate. As shown in Fig. 5 (section a–b), experiments first increased

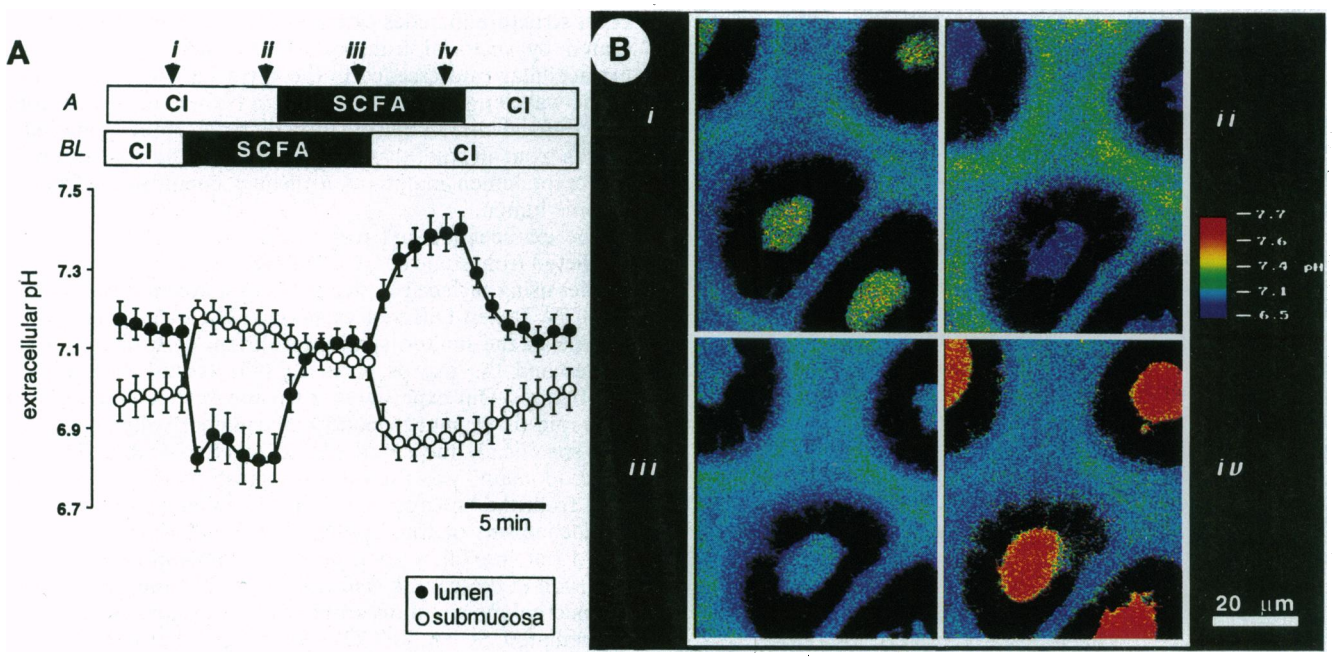

FIG. 3. Effect of transepithelial SCFA gradients on extracellular pH. (*A*) Time course of extracellular pH changes with separate results for measurement of luminal and submucosal pH, as in Fig. 2. Data are mean ± SEM ($n = 11$ crypts from three experiments) after crypts were exposed to sodium isobutyrate (SCFA) or NaCl (Cl) medium in apical (A) and/or basolateral (BL) perfusate. (*B*) Ratio images of colonic crypts from representative experiment performed as in *A*. Corresponding markers (*i–iv*) above the graph in *A* indicate times at which images were collected.

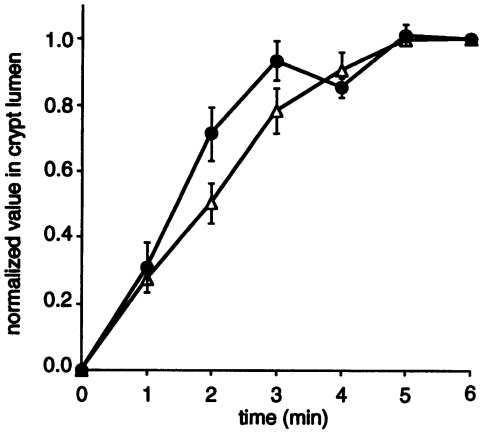

FIG. 4. Comparison of perfusate access to crypt lumen versus time course of luminal pH change caused by SCFAs. Experiments started with dye-free NaCl medium perfused at both tissue surfaces. SNARF-1 (0.1 mM) was added to apical NaCl perfusate and the appearance of 640-nm fluorescence was measured in crypt lumens at a single focal plane in *xy* images. After the dye equilibrated in the lumens (6 min), apical perfusate was changed to isobutyrate medium (containing 0.1 mM SNARF-1) and the time course of luminal pH change was monitored at the same location in the same crypts. To compare results between measurements of dye wash-in (△) and pH change (●), results are presented as the fractional change in each value observed over the time course: normalized value = $(X - X_i)/(X_f - X_i)$, where X_i = initial value prior to switch in perfusate, X_f = final value after perfusate switch, and X = data at intermediate time points. Results in figure are mean ± SEM (n = 7 crypts from four experiments) of normalized values.

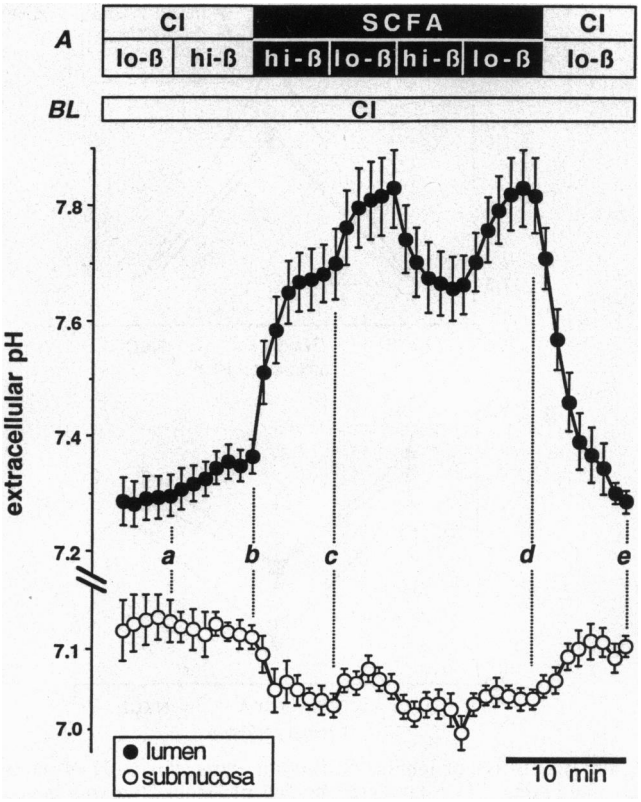

FIG. 5. Effect of apical perfusate buffering on crypt extracellular pH. Crypts were exposed to apical perfusates with variable buffering capacity but constant medium pH (low buffering capacity, Cl lo-β; high buffering capacity, Cl hi-β). Basolateral perfusate was standard NaCl medium (containing 20 mM Hepes) throughout the experiment. To examine the effects of SCFA, 100 mM sodium isobutyrate was substituted for 100 mM NaCl in either low or high buffering capacity formulation (SCFA lo-β and SCFA hi-β, respectively). Extracellular pH was measured in crypt lumen and submucosa as before. Results are mean ± SEM (n = 10 crypts from six experiments). Letters a–e guide discussion in text.

apical buffering capacity in chloride-containing medium, and luminal pH approached perfusate pH (7.4). Next, high buffering capacity was maintained while SCFA was added to apical perfusate (b–c), and then luminal buffering capacity was varied in the presence of constant [SCFA] (c–d). Results show (*i*) a reversible effect of varying buffering capacity in the presence of constant [SCFA] (pH changes within section c–d) and (*ii*) larger luminal pH change in the presence versus the absence of SCFAs (compare effects of switching buffering capacity within c–d versus a–b, respectively). These results show that SCFA gradients activate and sustain net flux of acid equivalents from the lumen.

Results in Fig. 5 also allow comparison of isobutyrate-induced pH changes when the same crypts were preequilibrated with high versus low buffering capacity. Comparison of pH changes in section b–c versus section d–e in Fig. 5 (high versus low buffering, respectively) indicates that luminal pH changes caused by isobutyrate differed by 1.9 ± 0.2-fold (n = 10). This value was 6-fold smaller than expected from measurements of medium buffering capacity (by direct titration of perfusates after use in experiments), which predicted an 11.7-fold difference over these pH ranges (data not shown). Results suggest that crypt colonocytes contribute significant pH buffering to luminal fluid. Assuming constant transepithelial flux of acid/base equivalents, results can be explained by colonic crypts contributing 33 mM H^+/pH unit of extracellular buffering capacity to the lumen. This upper estimate will be lowered if SCFA fluxes are inhibited by luminal alkalinization (6, 26, 27) or if perfusate buffers do not attain full concentration within the lumen.

DISCUSSION

Quantitative confocal microscopy has been applied to study colonic epithelium having intact epithelial architecture, to directly address questions about interrelationships between epithelial structure and function. Results suggest that colonic crypt structure includes extracellular microenvironments regulated by vectorial transport. One other group measured extracellular fluorescence in the crypt lumen (28), but these single-wavelength studies of SBFI (a Na-sensitive dye) from a nonconfocal microscope are difficult to interpret. Nonetheless, results from all studies are consistent with the conclusion that the crypt lumen maintains a distinct composition from the colonic lumen.

The extracellular pH response to apical SCFAs could be predicted from some (13, 15, 18), but not all (14, 19), previous studies using surface pH electrodes or mathematical modeling of SCFA fluxes. Differences among pH electrode results may be due to the limited spatial resolution of surface pH electrodes and the use of perfused (15) versus static (13, 14) incubations. Our experiments measured extracellular pH during rapid tissue superfusion (>20 chamber volumes per min) and specifically measured pH adjacent to crypts. The term "microdomain" was used to distinguish the spaces we evaluated from the "microclimate" at the colonic surface.

Mechanisms of transepithelial SCFA fluxes are being debated but are likely to include a combination of nonionic diffusion of these weak acids (9, 19, 26–28) and the activity of defined colonocyte monocarboxylate transporters (e.g., carrier-mediated $SCFA^-/HCO_3^-$ exchange and/or $SCFA^-/H^+$ cotransport) (29, 32). Simple models of transcellular SCFA fluxes via any of these transporters can explain our observations. As an example, in the presence of a physiologically oriented SCFA gradient, apical influx of SCFA via nonionic

diffusion could cause luminal alkalinization as protons are consumed (via reassociation of SCFA anion with protons) to fuel continuous nonionic uptake. Such alkalinization has been shown to occur in lipid bilayers (26). Nonionic SCFA efflux at the basal pole of the colonocyte could acidify submucosal pH due to the continued appearance and dissociation of protonated acid in that compartment. Related models may be envisioned based on the predicted net acid/base transport mediated by other SCFA transporters (29–32). However, our results require that any model must include (*i*) vectorial transepithelial acid/base transport, (*ii*) reversible transport mechanisms, (*iii*) a dependence on the presence and orientation of the transepithelial SCFA gradient, and (*iv*) sustained acid/base transport activated by a transepithelial SCFA gradient. Sustained transport is required to overcome abundant buffering in the crypt lumen (potentially contributed by proteins in the apical membrane of colonocytes, secreted mucins, or other unidentified substances).

The physiologic impact of microdomain extracellular pH regulation is not yet known. Most important, we have not defined the epithelial cell types exposed to the pH microdomains. The colonic crypt contains multiple epithelial cell types (1), but sites of ion absorptive and secretory functions along the crypt-to-surface axis are still being established (33–35). We speculate that extracellular pH regulation could contribute to several recognized effects of SCFAs on colonic ion transport. Polarized regulation of extracellular pH may help explain how polarized Na^+/H^+ exchangers are selectively activated by transepithelial SCFA gradients (8). Extracellular pH can regulate Na^+/H^+ exchange via competition between protons and the sodium substrate site (36); therefore luminal alkalinization should stimulate apical Na^+/H^+ exchange, and submucosal acidification should inhibit basal Na^+/H^+ exchange. In addition, regulation of extracellular pH will affect the pH-sensitive fraction of transepithelial SCFA absorption and may have confounded tissue experiments testing the pH sensitivity of SCFA transport (4, 6, 27, 37). The transepithelial pH gradient established by SCFAs is also a driving force for titration of other weak acids and bases across the epithelium, potentially explaining how SCFAs stimulate colonic bicarbonate secretion (38) and ammonia absorption (39). Further experiments are needed to substantiate these speculations, but it is clear that extracellular pH regulation has the potential to explain numerous effects of SCFAs.

All epithelia exist at interfaces between dissimilar environments. Our results show that tissue architecture and vectorial transport can directly contribute to regulating the microenvironment adjacent to epithelia. Extracellular regulation is predicted to be important for modifying epithelial transport function (8, 13, 15, 16, 18, 19) as well as providing a local regulatory mechanism to integratively control function among diverse cell types exposed to the microdomain. This demonstration of dynamic extracellular pH regulation in native tissue suggests further roles for the crypt lumen in maintaining a specialized environment and identifies a potential site for cellular regulation.

We are grateful to William Brownell for his remarkable generosity in providing us access to his confocal microscope (purchased with funds from the Office of Naval Research and the Hasselbad Foundation). We also thank Drs. Brownell, Bill Guggino, Mark Donowitz, and Chahrzad Montrose-Rafizadeh for critical reading of the manuscript. This work was supported by National Institutes of Health Grants R01 DK42457 and P01 DK44484.

1. Binder, H. J. & Sandle, G. I. (1994) in *Physiology of the Gastrointestinal Tract*, ed. Johnson, L. R. (Raven, New York), pp. 2133–2171.
2. Macfarlane, G. T. & Cummings, J. H. (1991) in *The Large Intestine: Physiology, Pathophysiology, and Disease*, eds. Philips, S. F., Pemberton, J. H. & Shorter, R. G. (Raven, New York), pp. 51–92.
3. Cummings, J. H., Pomare, E. W., Branch, W. J., Naylor, C. P. E. & Macfarlane, G. T. (1987) *Gut* **28,** 1221–1227.
4. Rübsamen, K. & Engelhardt, W. V. (1981) *Pflügers Arch.* **391,** 141–146.
5. Binder, H. J. & Mehta, P. (1989) *Gastroenterology* **96,** 989–996.
6. Gabel, G., Vogler, S. & Martens, H. (1991) *J. Comp. Physiol. B* **161,** 419–426.
7. Holtug, K. (1989) *Acta Vet. Scand.* **86,** 126–133.
8. Rowe, W. A., Lesho, M. J. & Montrose, M. H. (1994) *Proc. Natl. Acad. Sci. USA* **91,** 6166–6170.
9. Rowe, W. A., Blackmon, D. L. & Montrose, M. H. (1993) *Am. J. Physiol.* **265,** G564–G571.
10. Diener, M., Helmle-Kolb, C., Murer, H. & Scharrer, E. (1993) *Pflüglers Arch.* **424,** 216–223.
11. Desoigne, R. & Sellin, J. H. (1994) *Gastroenterology* **107,** 347–356.
12. Petersen, K.-U., Wood, J. R., Schulze, G. & Heintze, K. (1981) *J. Membrane Biol.* **62,** 183–193.
13. Holtug, K., McEwan, G. T. & Skadhauge, E. (1992) *Comp. Biochem. Physiol. A* **103,** 649–652.
14. Rechkemmer, G., Wahl, M., Kuschinsky, W. & Engelhardt, W. v. (1986) *Pflügers Arch.* **407,** 33–40.
15. Laverty, G., Holtug, K., Elbrønd, V. S., Ridderstråle, Y. & Skadhauge, E. (1994) *J. Comp. Physiol. B* **163,** 633–641.
16. Chatton, J.-Y. & Spring, K. R. (1994) *J. Membr. Biol.* **140,** 89–99.
17. Harris, P. J., Chatton, J.-Y., Tran, P. H., Bungay, P. M. & Spring, K. R. (1994) *Am. J. Physiol.* **266,** C73–C80.
18. Lucas, M. L. (1984) *Am. J. Physiol.* **247,** G463–G467.
19. Jackson, M. J., Williamson, A. M., Dombrowski, W. A. & Garner, D. E. (1978) *J. Gen. Physiol.* **71,** 301–327.
20. Montrose, M. H., Friedrich, T. & Murer, H. (1987) *J. Membr. Biol.* **97,** 63–78.
21. Bassnett, S., Reinisch, L. & Beebe, D. C. (1990) *Am. J. Physiol.* **258,** C171–C178.
22. Høverstad, T., Midtvedt, T. & Bøhmer, T. (1987) *Scand. J. Gastroenterol.* **20,** 373–380.
23. Weigand, E., Yound, J. W. & McGilliard, A. D. (1975) *J. Dairy Sci.* **58,** 1294–1300.
24. Annison, E. F. & Pennington, R. J. (1954) *Biochem J.* **57,** 685–692.
25. Roediger, W. E. W. (1982) *Gastroenterology* **83,** 424–429.
26. Gutknecht, J. & Tosteson, D. C. (1973) *Science* **182,** 1258–1261.
27. Sellin, J. H., DeSoignie, R. & Burlingame, S. (1993) *J. Membr. Biol.* **136,** 147–158.
28. Pedley, K. C. & Naftalin, R. J. (1993) *J. Physiol. (London)* **460,** 525–547.
29. Reynolds, D. A., Rajendran, V. M. & Binder, H. J. (1993) *Gastroenterology* **105,** 725–732.
30. Mascolo, N., Rajendran, V. M. & Binder, H. J. (1991) *Gastroenterology* **101,** 331–338.
31. Harig, J. M., Soergel, K. H., Barry, J. A. & Ramaswamy, K. (1991) *Am. J. Physiol.* **260,** G776–G782.
32. Garcia, C. K., Goldstein, J. L., Pathak, R. K., Anderson, R. G. W. & Brown, M. S. (1994) *Cell* **76,** 865–873.
33. Bookstein, C., Depaoli, A. M., Xie, Y., Niu, P., Musch, M. W., Rao, M. C. & Chang, E. B. (1994) *J. Clin. Invest.* **93,** 106–113.
34. Köckerling, A. & Fromm, M. (1993) *Am. J. Physiol.* **264,** C1294–C1301.
35. Diener, M., Rummel, W., Mestres, P. & Lindemann, B. (1989) *J. Membr. Biol.* **108,** 21–30.
36. Montrose, M. H. & Murer, H. (1988) in *Na^+/H^+ Exchange*, ed. Grinstein, S. (CRC, Boca Raton, FL), pp. 57–75.
37. Rönnau, K., Guth, D. & Engelhardt, W. v. (1989) *Q. J. Exp. Physiol.* **74,** 511–519.
38. Umesaki, Y., Yajima, T., Yokokura, T. & Masahiko, M. (1979) *Pflügers Arch.* **379,** 43–47.
39. Bödeker, D., Shen, Y., Kemkowski, J. & Höller, H. (1992) *Exp. Physiol.* **77,** 369–376.